Abscisic acid is an endogenous cytokine in human granulocytes with cyclic ADP-ribose as second messenger

Santina Bruzzone*[†], Iliana Moreschi*, Cesare Usai[‡], Lucrezia Guida*[†], Gianluca Damonte*, Annalisa Salis*, Sonia Scarfì*[†], Enrico Millo*, Antonio De Flora*, and Elena Zocchi*[†][§]

*Department of Experimental Medicine, Section of Biochemistry, and Center of Excellence for Biomedical Research, University of Genova, Viale Benedetto XV/1, 16132 Genoa, Italy; [†]Advanced Biotechnology Centre, Largo Rosanna Benzi 10, 16132 Genoa, Italy; and [‡]Institute of Biophysics, Consiglio Nazionale delle Ricerche, Via De Marini 6, 16149 Genoa, Italy

Abscisic acid (ABA) is a phytohormone involved in fundamental physiological processes of higher plants, such as response to abiotic stress (temperature, light, drought), regulation of seed dormancy and germination, and control of stomatal closure. Here, we provide evidence that ABA stimulates several functional activities [phagocytosis, reactive oxygen species and nitric oxide (NO) production, and chemotaxis] of human granulocytes through a signaling pathway sequentially involving a pertussis toxin (PTX)-sensitive G protein/receptor complex, protein kinase A activation, ADP-ribosyl cyclase phosphorylation, and consequent cyclic-ADP-ribose overproduction, leading to an increase of the intracellular Ca^{2+} concentration. The increase of free intracellular ABA and its release by activated human granulocytes indicate that ABA should be considered as a new pro-inflammatory cytokine in humans. This discovery is an intriguing example of conservation of a hormone and its signaling pathway from plants to humans and provides insight into the molecular mechanisms of granulocyte activation, possibly leading to the development of new antiinflammatory drugs.

inflammation | intracellular calcium

Abscisic acid (ABA) is a phytohormone regulating several important physiological functions in higher plants, including response to abiotic stress (temperature, light, drought), regulation of seed dormancy and germination, and control of stomatal closure (1). The functional effects induced by ABA are mediated by an increase of the intracellular calcium concentration ($[Ca^{2+}]_i$) involving the universal calcium mobilizer cyclic ADP-ribose (cADPR) (2, 3).

Recently, a number of observations indicate that a physiological role of ABA may not be restricted to Metaphyta. In lower Metazoa (Porifera, Hydrozoa), ABA synthesis is stimulated by environmental stimuli, such as temperature stress in marine sponges (4) and light exposure in hydroids (5). ABA activates ADP-ribosyl cyclase (ADPRC) through a protein kinase A (PKA)-mediated phosphorylation: ADPRC activation results in an increase of the intracellular cADPR concentration ($[cADPR]_i$), which induces intracellular Ca^{2+} release. The increase of the $[Ca^{2+}]_i$ stimulates oxygen consumption, protein synthesis, and water filtration in sponges (6), and stem cell-mediated tissue regeneration in hydroids (5). Thus, a signaling pathway relating cell functions to environmental conditions could be suggested as a common role of the ABA/cADPR system for both Metaphyta and Metazoa.

Granulocytes are the mammalian cell type perhaps most exposed to environmental stimuli, being the first line of defense against pathogens. Circulating granulocytes can rapidly extravasate in response to chemotactic stimuli, and their phagocytic activity, together with the ability to produce cytotoxic reactive oxygen species (ROS) and nitric oxide (NO), results in killing of the pathogens. A severe reduction of the number of circulating granulocytes (as occurs in aplastic anemia syndromes, in certain leukemias, and during the first weeks after bone marrow transplant) or a malfunctioning of the process of phagocytosis/killing (as occurs in some genetic diseases) cause severe and recurrent infections, burdened by a high mortality rate. All of the above-mentioned functions of granulocytes are dependent on an increase of the $[Ca^{2+}]_i$, although in most cases, the underlying molecular mechanisms are unknown. Involvement of cADPR in the regulation of granulocyte function was unequivocally demonstrated by Partida-Sánchez et al. (7), who showed that deletion of the mammalian ADPRC CD38 renders mice susceptible to *Streptococcus pneumoniae* infection because of the failure of their neutrophils to migrate to the infected lung tissue. This functional impairment of the $CD38^{-/-}$ neutrophils is caused by absence of the cADPR-induced $[Ca^{2+}]_i$ increase. In addition, cADPR has been shown to regulate chemotaxis in human granulocytes and monocytes in response to different stimuli through a $[Ca^{2+}]_i$ increase (8, 9).

We explored the possibility that ABA may affect human granulocyte function by modifying the $[Ca^{2+}]_i$. The present results indicate that addition of ABA, at concentrations ranging from 50 nM to 20 μM, indeed stimulates phagocytosis, ROS and NO production, chemotaxis, and chemokinesis. The signaling pathway triggered by ABA in granulocytes involves engagement of a PTX-sensitive receptor/G protein complex, activation of adenylyl cyclase (AC), cAMP overproduction, and PKA-mediated phosphorylation of the ADPRC CD38. ADPRC activation then leads to increased $[cADPR]_i$ and $[Ca^{2+}]_i$. Presence of ABA in human granulocytes, the increase of the intracellular free ABA concentration after heat-stress, and its release triggered by phagocytosis indicate that ABA should be regarded as a new endogenous proinflammatory cytokine in humans.

Results and Discussion

ABA Induces a Sustained Ca^{2+} Response in Human Granulocytes, with cADPR and IP_3 as Second Messengers. Freshly isolated, Fura-2-loaded granulocytes were incubated with ($\pm$)-cis, trans ABA

BIOCHEMISTRY

Fig. 1. ABA increases the $[Ca^{2+}]_i$ in FURA-2-AM loaded human granulocytes. (*A*) ABA (20 μM) was added to cells in HBSS (trace 1) or in Ca^{2+}-free HBSS containing 0.1 mM EGTA (trace 2). (*B*) ABA (20 μM) was added to untreated cells in HBSS (trace 1), to cells pretreated with xestospongin (10 μM for 10 min) (trace 2), with U73122 (5 μM for 10 min) (trace 3), with 8-Br-cADPR (100 μM for 90 min) (trace 4), with both U73122 and 8-Br-cADPR (trace 5), or with PTX (2 μg/ml for 1 h) (trace 6). Traces from one of three different experiments, yielding comparable results, are shown. Arrows indicate the addition of ABA.

(henceforth called ABA) in Hanks' balanced salt solution (HBSS) buffer: a concentration of 0.1 μM ("molar" always indicating final concentrations) was sufficient to induce an immediate and sustained $[Ca^{2+}]_i$ increase. After 10 min from the addition of 0.1, 1 and 20 μM ABA, the $[Ca^{2+}]_i$ increased from a basal value of 50 ± 3 to 62 ± 5, 73 ± 4, and 102 ± 6 nM, respectively ($n = 5$, $P < 0.05$ for 0.1 and 1 μM; $P < 0.0001$ for 20 μM). Prolonging the incubation time (up to 45 min) resulted in a further slight increase of the $[Ca^{2+}]_i$, suggesting that a plateau was reached. To assess the specificity of the Ca^{2+} response to ABA, several compounds structurally similar to ABA [see supporting information (SI) Fig. 5*A*] were tested. The ABA enantiomers (+)- and (−)-ABA were similarly effective (data not shown), whereas the Ca^{2+} increase observed with 20 μM ($\pm$)-trans, trans ABA ($\approx$25% of that recorded with 20 μM cis, trans ABA) was similar to that induced by contaminant ($\leq$0.5%) cis, trans ABA (see SI Fig. 5*B*) still present after HPLC purification of trans, trans ABA. ABA-methylamide and trans, trans retinoic acid at 20 μM did not induce any Ca^{2+} increase (see SI Fig. 5*B*).

When ABA was added to granulocytes in the presence of extracellular EGTA in Ca^{2+}-free HBSS, the sustained Ca^{2+} elevation was strongly reduced (by $\approx$80%) (Fig. 1*A*, trace 2), demonstrating that influx of extracellular Ca^{2+} is primarily responsible for the generation of the ABA-induced $[Ca^{2+}]_i$ increase.

To investigate a possible role of cADPR in this Ca^{2+} response, intact granulocytes were exposed to ABA after preincubation with either 8-Br-cADPR, a membrane-permeant cADPR antagonist (10), or ryanodine at a concentration known to inhibit Ca^{2+} release from cADPR-responsive stores (11). Both 8-Br-cADPR (Fig. 1*B*, trace 4) and ryanodine (data not shown) almost abolished the ABA-induced $[Ca^{2+}]_i$ increase, whereas they did not affect the Ca^{2+} rise triggered by IL-8 (see SI Fig. 5*C*), which is known to induce Ca^{2+} signaling in neutrophils via a pathway not involving cADPR (8). In line with this result, a minor role of IP_3 in the ABA-induced $[Ca^{2+}]_i$ rise was demonstrated by the effect of 10 μM xestospongin, a specific IP_3 antagonist acting on the corresponding receptor channel (12), which decreased the $[Ca^{2+}]_i$ elevation by $\approx$15% (Fig. 1*B*, trace 2). Higher concentrations of xestospongin did not further decrease the ABA-induced Ca^{2+} increase.

Preincubation of intact granulocytes with the membrane-permeant phospholipase C (PLC) inhibitor U73122 (5 μM) significantly reduced (by $\approx$40%, $n = 3$) the $[Ca^{2+}]_i$ rise induced by 20 μM ABA (Fig. 1*B*, trace 3), whereas the same concentration of the inactive analogue U73343 was ineffective (data not shown). Increasing the concentration of U73122 did not further reduce the $[Ca^{2+}]_i$ rise. The higher percentage of inhibition afforded by U73122 compared with xestospongin suggests the involvement of the other product of PLC beside IP_3, i.e.,

diacylglycerol, in the signaling pathway triggered by ABA and leading to the $[Ca^{2+}]_i$ increase. Presence of either 8-Br-cADPR or ryanodine together with U73122 resulted in the abrogation of the ABA-induced $[Ca^{2+}]_i$ rise (Fig. 1*B*, trace 5), as also observed when intact granulocytes were preincubated with PTX before ABA challenge (Fig. 1*B*, trace 6).

Involvement of both cADPR and IP_3 in the ABA-induced calcium response was confirmed by the increase of their intracellular concentration after granulocyte stimulation with 20 μM ABA (Fig. 2 *A* and *B*). The $[IP_3]_i$ increase was less extensive and occurred with a very different time-course (Fig. 2*B*). Preincubation of granulocytes with PTX resulted in the complete inhibition of the ABA-induced increase of the $[cADPR]_i$ and of the $[IP_3]_i$ (Fig. 2 *A* and *B*, rhombus).

ABA Stimulates ADPRC Activity in Granulocytes. Involvement of cADPR in the ABA-induced Ca^{2+} increase in granulocytes prompted us to investigate the effect of ABA on the ADPRC activity, which in these cells is expressed by the transmembrane ectoenzyme CD38 (7). In intact granulocytes exposed to 20 μM ABA, the ectocellular ADPRC activity increased by 70% 5 min after addition of ABA (SI Table 1). Conversely, NAD^+-ase and cADPR-hydrolase activities, coexpressed by CD38 together with the cyclase activity (13), were not significantly modified by ABA (see SI Table 1). Granulocyte GDP-ribosyl cyclase (GDPRC) activity on NGD^+ (a NAD^+ analogue yielding the poorly hydrolyzed cyclic product cGDPR), as measured on intact cells, also increased by $\approx$80% 5 min after addition of 20 μM ABA, in agreement with the similar percentage of increase observed for the ADPRC activity. In Fig. 2*C*, the percentage of increase of both ADPRC and GDPRC activities in ABA-stimulated cells relative to controls is shown as a function of time: activation was highest after 5 min incubation with ABA (180% of control values), and cyclase activity remained up-regulated for at least 2 h. The kinetics of activation of the GDPRC and ADPRC activities were similar. Submicromolar ABA concentrations also stimulated GDPRC activity: the average between the GDPRC values recorded after 5- and 15-min incubation of the cells with ABA increased by 23%, 30%, 38%, and 60% in the presence of 50 nM, 250 nM, 1 μM, and 5 μM ABA, respectively ($n = 6$, $P < 0.05$). The percentage of increase of the cyclase activity at 5 μM ABA was similar to that obtained with 20 μM ABA.

Role of PKA in the ABA-Induced Activation of ADPRC Activity. To investigate a possible role of protein kinases in the ABA-induced ADPRC activation in human granulocytes, cells were preincubated with K252a, a general protein kinase inhibitor, or with a PKA-specific myristoylated peptide (cell-permeant), or with a PKC-specific inhibitor before the addition of ABA. The increase of the cyclase activity on NGD^+ induced by 20 μM ABA was completely abrogated by either K252a or the PKA inhibitor (SI Fig. 6), indicating a principal role of PKA in ABA-induced A(G)DPRC phosphorylation. Indeed, the increase of the $[cADPR]_i$ induced by ABA was prevented by pretreatment of granulocytes with the PKA-specific inhibitor (Fig. 2*A*, triangles). The PKC inhibitor also induced a significant inhibition of the A(G)DPRC activity (58%) (SI Fig. 6*A*), which suggests a role also for PKC in the signaling pathway, upstream of PKA. Finally, preincubation of granulocytes with PTX prevented the ABA-induced A(G)DPRC activation (SI Fig. 6*A*), confirming the involvement of a PTX-sensitive G protein in the ABA-signaling pathway leading to the $[cADPR]_i$ increase (Fig. 2*A*, rhombus).

The level of phosphorylation of CD38 in ABA-stimulated granulocytes was also investigated. In preliminary experiments, intact cells were preincubated for 10 min in the presence or absence of 20 μM extracellular ABA. The cyclase activity of the cell lysates was up-regulated to an extent similar to that measured on intact cells (0.155 ± 0.016 vs. 0.258 ± 0.020 nmol of
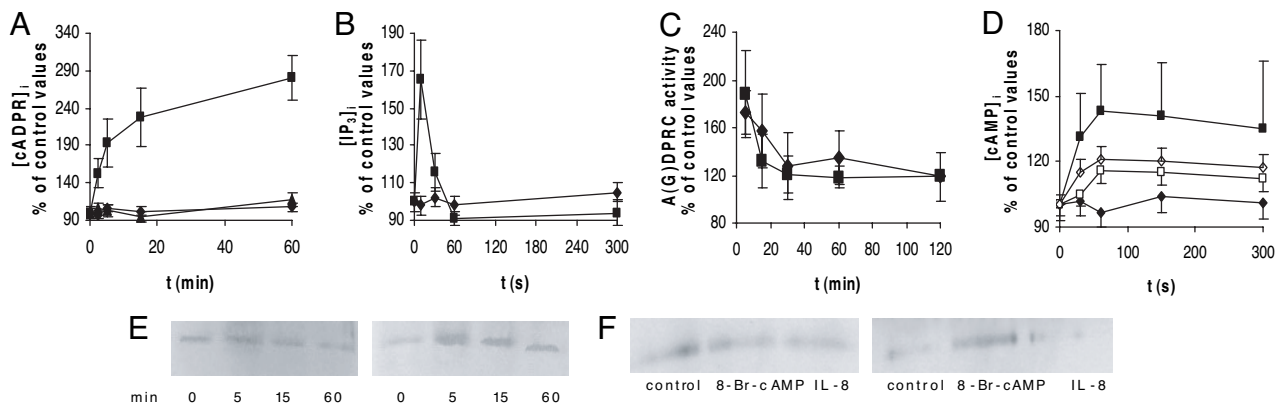
Fig. 2. Intracellular cADPR, IP$_3$ and cAMP levels, ADPRC activity, and CD38 phosphorylation in ABA-stimulated granulocytes. (*A*) After addition of 20 μM ABA, [cADPR]$_i$ levels were determined on untreated cells (squares, $n = 9$), or on cells pretreated with a specific PKA inhibitor (10 μM for 15 min) (triangles, $n = 3$) or with PTX (2 μg/ml for 1 h) (rhombus, $n = 3$). The basal [cADPR]$_i$ recorded in unstimulated cells was 31.48 $\pm$ 14.15 pmol/10^9 cells, $n = 9$. (*B*) [IP$_3$]$_i$ levels were determined on untreated cells (squares, $n = 4$) or on cells pretreated with PTX (2 μg/ml for 1 h) (rhombus, $n = 4$). The basal [IP$_3$]$_i$ measured in unstimulated cells was 1.32 $\pm$ 0.44 pmol/10^6 cells, $n = 4$. (*C*) ADP- (rhombus) and GDP- (square) ribosyl cyclase activities. (*D*) [cAMP]$_i$ levels were determined on untreated cells (filled squares, $n = 20$), on cells pretreated with PTX (2 μg/ml for 1 h) (filled rhombus, $n = 3$), with U73122 (5 μM for 10 min) (opened squares, $n = 3$), or with a specific PKC inhibitor (50 nM for 15 min) (white rhombus, $n = 4$). Higher concentrations of U73122 and of the PKC inhibitor did not further increase the percentage of inhibition. Results are expressed as percentage of basal values, recorded on untreated cells. (*E* and *F*) CD38 was immunopurified (see *SI Materials and Methods*) as follows: from ABA-treated (for 0, 5, 15, and 60 min with 20 μM ABA) granulocytes (*E*) and from control, 8-Br-cAMP- (500 μM for 15 min) and IL-8- (100 nM for 15 min) treated granulocytes (*F*). Samples were run in duplicate; Western blots were stained with the anti-CD38 antibody (*Left*) or with an anti-phosphoserine mAB (*Right*). Results from one of three different experiments, yielding comparable results, are shown.

cGDPR/min/mg in control and ABA-pretreated cells, respectively, as recorded after 15 min incubation of the intact cells with 20 μM ABA; $n = 3$, $P < 0.005$), indicating that the ABA-induced protein modification was preserved after cell lysis. Next, CD38 was immunopurified from lysates of control and of ABA-stimulated cells: detection with an anti-phosphoserine monoclonal antibody (mAB) revealed a more intense protein band, at the molecular mass expected for CD38 in the ABA-treated sample compared with the control (SI Fig. 6*B*), thus demonstrating a higher proportion of phosphorylated protein in ABA-treated cells. The time course indicated that CD38 phosphorylation was maximal at 5 min (Fig. 2*E*), in line with the assay of A(G)DPRC activity (Fig. 2*C*).

PKA-mediated activation of ADPRC has already been shown to occur upon exposure of granulocytes to 8-Br-cAMP (a cell-permeant PKA activator), with both the ADPRC activity and the [cADPR]$_i$ levels being increased (9). The 8-Br-cAMP-induced increase of the [cADPR]$_i$ was also paralleled by a sustained 8-Br-cADPR-inhibitable [Ca^{2+}]$_i$ increase (9), similar to that observed in this study with ABA. Indeed, 8-Br-cAMP induced a similar extent of CD38 phosphorylation as ABA (Fig. 2*F*), whereas cell preincubation with IL-8, which is known to induce Ca^{2+} signaling in neutrophils via a pathway not involving CD38 and cADPR (8), did not result in CD38 phosphorylation (Fig. 2*F*).

Taken together, these results indicate a causal role of PKA in the activation of granulocyte ADPRC by ABA. ABA has indeed been demonstrated to activate ADPRC by means of a protein kinase in plants and sponges (3, 4), and PKA was specifically involved in the ABA-induced signaling pathway in hydroids (5). In all these cases, cyclase phosphorylation resulted in an increase of the [cADPR]$_i$.

Mechanisms of Activation of AC in ABA-Stimulated Granulocytes. To conclusively demonstrate a role of PKA in the ABA-induced ADPRC activation, we investigated whether ABA treatment induced an increase of the intracellular cAMP concentration ([cAMP]$_i$). Indeed, the basal [cAMP]$_i$ of human granulocytes (1.66 $\pm$ 0.51 pmol/10^6 cells, $n = 20$) increased immediately after stimulation with 20 μM ABA (Fig. 2*D*). The ABA enantiomers

(+)- and (−)-ABA were similarly effective. Conversely, ABA-methylamide, at 20 μM, did not induce any [cAMP]$_i$ increase, and the slight [cAMP]$_i$ rise observed with 20 μM ($\pm$)-trans, trans ABA ($\approx$30% of that measured with 20 μM cis, trans ABA) could be attributed to contamination ($\leq$0.5%) by cis, trans ABA (data not shown), demonstrating the specificity of the effect of ABA.

Thus, cAMP generation and consequent PKA activation represent early steps in the signaling cascade triggered by ABA and leading to stimulation of ADPRC activity.

Rat and human neutrophils express both Ca^{2+}/calmodulin- and G protein/PKC-activated AC isoforms (14, 15). Presence of 0.3 mM extracellular EGTA did not modify the increase of the [cAMP]$_i$ induced by ABA (data not shown), thus ruling out activation of the AC and/or of PKC by influx of extracellular Ca^{2+}. Conversely, pretreatment of granulocytes with PTX or with a permeant PKC-specific inhibitor prevented or strongly reduced (by 47%) the ABA-induced [cAMP]$_i$ elevation, respectively (Fig. 2*D*), whereas the PKA inhibitor was without effect (data not shown). These results indicate that a PTX-sensitive G protein and PKC lie upstream of the AC-catalyzed [cAMP]$_i$ increase leading to PKA activation.

The partial inhibition of the ABA-induced [Ca^{2+}]$_i$ increase afforded by the PLC inhibitor U73122 (Fig. 1*B*) suggested to explore whether up-regulation of the [cAMP]$_i$ was also affected by U73122: indeed, preincubation with the PLC inhibitor reduced the ABA-triggered [cAMP]$_i$ elevation by 61% (Fig. 2*D*). This finding suggests a role for PLC, likely by its other product diacylglycerol, in the PKC-induced AC activation. Preincubation of granulocytes with PTX before ABA stimulation abrogated IP$_3$ synthesis (Fig. 2*B*), indicating the involvement of a PTX-sensitive G protein in the ABA-induced PLC activation.

Binding of ABA to Human Granulocytes. PTX abrogated all biochemical changes triggered by extracellular ABA, which suggests the occurrence of ABA receptor sites on the plasmamembrane of human granulocytes. Biotinylated ABA (bio-ABA) has been used to demonstrate presence of ABA-binding sites on the plasmamembrane of ABA-sensitive stomatal guard cells in plants (16). Bio-ABA induced the same [Ca^{2+}]$_i$ response on granulocytes as unmodified ABA (data not shown). Thus,

granulocytes were incubated with bio-ABA and subsequently with FITC-conjugated streptavidin: surface fluorescence was indeed detectable (SI Fig. 7 A and C), and excess unconjugated ABA completely prevented cell staining (SI Fig. 7 B and D). Presence of ABA-binding sites in human granulocytes was confirmed also with radioactive ABA. Intact cells were incubated with [^{3}H]-ABA at increasing concentrations, in the presence or absence of excess unlabeled ABA. Scatchard plot analysis of the results indicated presence of high- (SI Fig. 8A) and low-affinity (SI Fig. 8B) ABA-binding sites in intact human granulocytes. The K_d of the high-affinity binding site was 11 nM, similar to that described for ABA-binding proteins in plants (16–19), and the number of ABA-binding sites per cell (B_{max} = 6,000) was similar to that reported for G protein linked chemokine receptors in granulocytes (20). The K_d of the low-affinity binding site (K_d = 500 μM) was several logs higher than that of the high-affinity binding site, indicating that these binding sites are most likely not involved in ABA binding and signaling at the concentrations used in this study (50 nM to 20 μM). Taken together, these results indicate that ABA-binding sites occur on the surface of human granulocytes, although influx of ABA into granulocytes and interaction with intracellular receptor(s) cannot be ruled out. In plants, both intracellular and cell surface ABA-binding sites have been described (16–19), but neither receptor type has been as yet molecularly identified, with the exception of an RNA-binding nuclear protein recently demonstrated to bind ABA $in vitro$ (21). In plants, a significant proportion of intracellular ABA is conjugated to glucosyl groups (22): the very high number of low-affinity ABA binding sites per cell in granulocytes (B_{max} = 6 × 10^7) suggests the possibility that they represent similar intracellular storage forms of ABA and/or of ABA catabolites.

A schematic representation of the ABA signaling pathway in human granulocytes is shown in Fig. 3. The first event induced by exogenous ABA in human granulocytes is activation, supposedly through interaction at a transmembrane binding site, of PTX-sensitive G protein(s), as demonstrated by toxin-mediated inhibition of the ABA-induced increase of [IP$_3$]$_i$, [cAMP]$_i$, [cADPR]$_i$ (Fig. 2), and [Ca^{2+}]$_i$ (Fig. 1B). Activation of both PLC and AC follows, which induces a rapid increase of the [IP$_3$]$_i$ and [cAMP]$_i$ (Fig. 2 B and D). The PLC-dependent, diacylglycerol-induced PKC activation contributes to AC stimulation (Fig. 2D). The enhanced [cAMP]$_i$ levels activate PKA, leading to CD38 phosphorylation (Fig. 2E) and to the rapid up-regulation of its ADPRC activity (Fig. 2C), which is prevented by PTX and by the PKA-specific inhibitor (SI Fig. 6). A role of PKC in the direct activation of ADPRC seems to be ruled out by the complete absence of CD38 activation observed with the PKA-inhibitor alone (SI Fig. 6). ADPRC stimulation in turn results in an increase of the [cADPR]$_i$, which can be prevented by PTX and by the PKA-specific inhibitor (Fig. 2A). The increase of [cADPR]$_i$ induces an influx of extracellular Ca^{2+} (23) through either or both of the following mechanisms: (i) Ca^{2+} release from ryanodine receptor-gated stores, in turn activating store-operated Ca^{2+} entry (Fig. 3, path a), or (ii) direct cADPR-mediated opening of plasmamembrane Ca^{2+} channels (Fig. 3, path b). These mechanisms have been advocated also in the response of human granulocytes to extracellular NAD$^+$ (9) and of murine granulocytes to fMLP (7).

Presence on human granulocytes of TRPM2 channels gated by ADPR (24) suggests a possible role for ADPR, produced by the NAD$^+$-ase activity of CD38, in the ABA-induced Ca^{2+} increase. However, the following results rule out a significant contribution of ADPR to the Ca^{2+} signaling triggered by ABA: (i) the almost complete inhibition (80%) of the [Ca^{2+}]$_i$ rise afforded by 8-Br-cADPR (Fig. 1B), and (ii) activation of ADPRC, but not of NAD$^+$-ase or of cADPR hydrolase activities of CD38 by PKA (SI Table 1). However, at present, we cannot rule out a role of
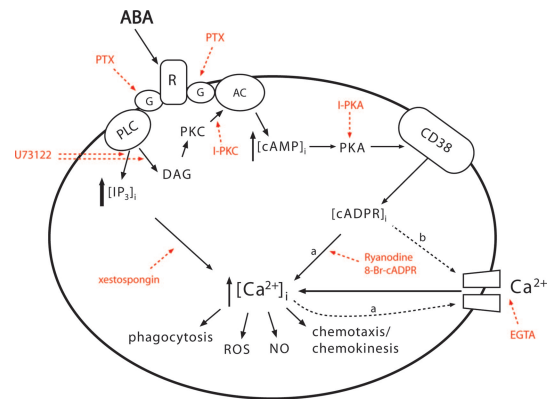
Fig. 3. Mechanism of the ABA-induced [Ca^{2+}]$_i$ increase. The interaction of ABA with a G protein-coupled plasmamembrane receptor triggers is shown as follows: (i) activation of PLC, overproduction of IP$_3$, and stimulation of a PKC-dependent AC; (ii) activation of AC, overproduction of cAMP, PKA-mediated stimulation of ADPRC, and increase of [cADPR]$_i$. Downstream of cADPR, two mechanisms (dotted lines) might cooperate to induce the observed increase of the [Ca^{2+}]$_i$: extracellular Ca^{2+} influx through store-operated Ca^{2+} entry (a) or direct gating of a plasmamembrane Ca^{2+} channel by cADPR (b). Site-specific inhibitors of the ABA-signaling pathway are indicated in red. PTX, pertussis toxin; U73122, PLC inhibitor; xestospongin, IP$_3$-specific Ca^{2+}-channel blocker; I-PKA and I-PKC, PKA- and PKC-specific myristoylated (peptide inhibitors); 8-Br-cADPR, specific cADPR antagonist; Ry, Ryanodine (cADPR-specific Ca^{2+}-channel blocker). The increased [Ca^{2+}]$_i$ levels stimulate functional responses: phagocytosis, release of ROS and NO, chemokinesis, and chemotaxis to ABA.

cADPR in the opening of the following TRPM2 channels: 8-Br-cADPR-inhibitable gating of these channels by cADPR has been described, albeit at high micromolar (100 μM) cADPR concentrations (25).

A major role of IP$_3$ in the intracellular Ca^{2+} release and in a subsequent store-operated Ca^{2+} entry can be ruled out by the very limited reduction of the Ca^{2+} rise (15%) elicited by the IP$_3$ receptor inhibitor xestospongin (Fig. 1B). Indeed, the increase of the [IP$_3$]$_i$ induced by ABA ($\approx$165% of control values) (see Fig. 2B) was significantly less than that observed in parallel experiments with fMLP (465 $\pm$ 45% of control values, n = 4), which is known to activate granulocytes primarily via PLC (26). This could account for the absence, in the ABA-induced Ca^{2+} rise, of the transient initial Ca^{2+} peak typical of an IP$_3$-induced Ca^{2+} rise.

The higher percentage of inhibition of the ABA-triggered [Ca^{2+}]$_i$ increase observed with the PLC inhibitor U73122 compared with xestospongin is in agreement with the proposed synergism of AC activation by the PTX-sensitive G protein and PKC (U73122 and PKC inhibitor both reduced the ABA-induced [cAMP]$_i$ increase, Fig. 2D).

The fundamental role of Ca^{2+} movements in granulocyte activation prompted us to explore the effect of ABA on some of the most relevant physiological functions of these cells. Indeed, a Ca^{2+} rise similar in extent and kinetics to that induced by ABA is triggered in human granulocytes by extracellular NAD$^+$ and stimulates ROS and NO production and chemotaxis (9).

ABA Stimulates Phagocytosis, ROS and NO Production, Chemotaxis, and Chemokinesis in Human Granulocytes. Human granulocytes were preincubated with ABA at concentrations ranging from 50 nM to 20 μM at 20°C for 15 min, and phagocytosis of fluorescent latex beads was evaluated at different times. ABA concentrations as low as 50 nM significantly stimulated phagocytosis. At a concentration of 20 μM, ABA markedly increased phagocytosis and PTX-pretreatment of the cells completely prevented this effect (SI Fig. 9A).

Bruzzone $et al.$

The addition of 20 μM ABA induced a six-fold increase of ROS production over control, unstimulated granulocytes, as detected over a 10 min-incubation time. PTX and 8-Br-cADPR abrogated the ABA-induced increase of ROS production (SI Fig. 9B).

ABA also significantly stimulated NO generation by human granulocytes, although a high variability in the extent of the increase over basal values was recorded among different subjects. NO generation by ABA-stimulated (20 μM) granulocytes, expressed as percentage of the production by unstimulated cells, ranged from 183 to 942, with a median value of 355 ($n = 8$) (SI Table 2). SI Fig. 9C shows the dose-dependence of the ABA-stimulated NO generation in neutrophils from a "low-" (black bars) and a "high-responder" (white bars) subject. The complete abrogation of the ABA-induced stimulation by extracellular EGTA (0.3 mM) and by EGTA-AM (50 μM) (data not shown) confirmed the causal role of Ca^{2+} in the ABA-induced NO generation. We also tested the effect on NO generation of a number of compounds known to interfere at various sites in the ABA signaling cascade. Preincubation of granulocytes with 100 μM 8-Br-cADPR, or with 50 μM ryanodine, or with 20 mM nicotinamide (an inhibitor of ADPRC activity), prevented or significantly reduced nitrite production in the ABA-stimulated cells (by 100%, 72%, and 97%, respectively, mean of the values determined on subjects 5, 6, and 7 of SI Table 2).

Inhibition by PTX, 8-Br-cADPR, and ryanodine of the ABA-induced stimulation of granulocyte phagocytosis and ROS and NO production indicates that these functional effects are downstream of a signaling pathway involving a PTX-sensitive receptor/G protein complex and cADPR as second messenger.

Different concentrations of ABA, placed in the bottom well of a chemotaxis migration chamber, induced a dose-dependent chemotactic response, with maximal migration being recorded toward 20 μM ABA and with as low as 50 nM ABA significantly increasing cell migration compared with controls (SI Fig. 9D). Similarly to NO production, a different sensitivity of the chemotactic response to ABA was also observed in granulocytes from different subjects. The median value of the CI toward ABA was 2.63 (range 1.51–6.44, $n = 5$) (SI Table 3). Similarly to what observed on the $[Ca^{2+}]_i$ and on the $[cAMP]_i$ increase, (+)- and (−)-ABA were as effective as ABA in stimulating chemotaxis. Conversely, ABA-methylamide, at 20 μM, did not induce any chemotactic response, and the limited migration observed toward 20 μM ($\pm$)-trans, trans ABA ($\approx$25% of that recorded toward 20 μM cis, trans ABA) could be attributed to contaminant ($\leq$0.5%) cis, trans ABA (data not shown), demonstrating the specificity of the effect of ABA on functional activation of granulocytes.

To assess the effect of ABA on chemokinesis (i.e., untargeted cell movement), granulocytes were first preincubated with 20 μM ABA and then placed on top of the filter of a chemotaxis chamber containing buffer in the bottom wells: cell migration through the filter was slightly (chemokinesis index = 1.3, $n = 3$) but consistently increased in ABA-treated cells compared with untreated controls (data not shown). In one of four experiments, the chemokinesis was greatly enhanced after ABA preincubation (chemokinesis index = 2.5).

Preincubation of cells with PTX, or 8-Br-cADPR or 50 μM ryanodine (data not shown), before exposure to ABA, abrogated chemotaxis (SI Fig. 9D) and chemokinesis (data not shown) induced by ABA; moreover, the simultaneous addition of 20 mM nicotinamide with ABA completely inhibited ABA-stimulated chemokinesis (data not shown). Conversely, preincubation of granulocytes with 100 μM 8-Br-cADPR, 50 μM ryanodine, or 20 mM nicotinamide did not affect cell migration toward IL-8 (data not shown), which is known to stimulate chemotaxis in human granulocytes via a pathway not involving CD38/cADPR (8).

These results indicate engagement of a PTX-sensitive recep-
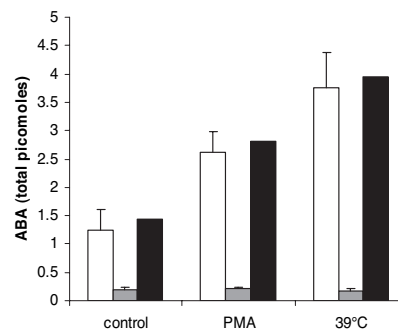
Fig. 4. Effect of PMA and temperature on granulocyte ABA content. Cells (5×10^7/determination) were incubated in 2.0 ml of HBSS for 30 min at 39°C or at 20°C without (control) or with PMA. The ABA content in cells and supernatants was determined by HPLC-MS. Results are expressed as picomoles of ABA detected in the cells (white bars) or in the supernatants (gray bars). Results shown are mean values $\pm$ SD ($n = 3$ for PMA, $n = 9$ for temperature) of granulocytes from different subjects. Black bars, sum of mean values of intracellular and released ABA.

tor/G protein complex and involvement of the cADPR/$[Ca^{2+}]_i$ signaling cascade in the migration response of granulocytes to ABA.

ABA in Human Granulocytes. Free ABA was detected by HPLC-MS (SI Fig. 10) in acid extracts of unstimulated human granulocytes at 0.23 $\pm$ 0.09 pmol/mg protein ($n = 9$). A fraction (30%) of the total ABA content was present as alkali-hydrolyzable, conjugated ABA, as also described in plants (22) and the mammalian brain (27). Presence of conjugated ABA in granulocytes supports the hypothesis that the low affinity binding sites (SI Fig. 8B) may represent intracellular storage forms of the hormone. The free $[ABA]_i$ increased in granulocytes challenged with chemical stimuli or exposed to fever-like temperatures: in cells incubated for 30 min at 20°C in the presence of 0.1 μg/ml PMA, the $[ABA]_i$ increased 2.1 $\pm$ 0.3-fold ($n = 3$) compared with controls; a slightly higher increase (3.0 $\pm$ 0.5 fold, $n = 3$) was observed in cells incubated for 30 min at 39°C (Fig. 4A). Granulocyte uptake of ABA from the medium during these incubations can be ruled out, because of the verified absence of ABA in the HBSS used in these experiments. No ABA release into the medium was observed after granulocyte incubation with PMA or at 39°C (Fig. 4). Conversely, the $[ABA]_i$ decreased and ABA was released extracellularly by granulocytes stimulated with zymosan or with latex bead (SI Fig. 11), as measured with a sensitive and specific ELISA kit (4, 5). The sum of the intra- and extracellular ABA content increased in particle-stimulated cells compared with controls suggests that ABA release is sustained by its intracellular production.

ABA release from particle-stimulated granulocytes suggested a possible autocrine role of endogenous ABA in stimulating ROS production triggered by phagocytosis. Removal of released ABA from the supernatant of particle-stimulated granulocytes should then reduce ROS production. To test this hypothesis, granulocytes (10^5 cells per assay, loaded with the ROS-specific fluorescent probe H_2DCFDA) were preincubated for 15 min without (control) or with 0.1 μg/ml of an anti-ABA mAB (Agdia, Elkhart, IN) and then challenged with zymosan (0.37 mg/ml). The fluorescence increase during the first 5 min was reduced by 80% in the mAb-treated cells compared with controls, and the addition of 20 μM ABA to mAb-treated cells restored ROS production to control levels ($n = 3$; data not shown).

These results demonstrate that ABA behaves as a proinflammatory endogenous cytokine capable of stimulating granulocyte functions (phagocytosis, ROS and NO production, che-

BIOCHEMISTRY

motaxis, and chemokinesis) through a signaling pathway involving a PTX-sensitive receptor/G protein complex, PLC activation, PKA-mediated ADPRC phosphorylation, and cADPR overproduction, eventually leading to an increase of the $[Ca^{2+}]_i$.

These signaling steps show striking similarities with the plant and sponge ABA signaling pathways. In plants, ABA is known to trigger PLC activation via a G protein-linked receptor (28) and to activate ADPRC leading to cADPR overproduction, $[Ca^{2+}]_i$ increase, gene transcription, and stomatal closure (3). In sponges, ABA triggers PKA-dependent ADPRC phosphorylation and cADPR-mediated $[Ca^{2+}]_i$ increase, leading to stimulation of water filtration and oxygen consumption (4, 6).

The demonstration of a role of ABA in inflammation will bear far-reaching consequences in several scientific aspects. From the evolutionary point of view, it is the first example of conservation of a hormone and its significance as a stress signal and its transduction pathway from plants to mammals; from a clinical perspective, identification of a new inflammation cytokine will improve our knowledge of the physiology of inflammation, possibly leading to the development of new antiinflammatory drugs.

Inflammatory chemokines have been recently proposed as a new major family of neuromodulators along with neurotransmitters and neuropeptides (29, 30). Interestingly, ABA (free and conjugated) has been detected in the brain of vertebrates (27), suggesting a whole new area of investigation into the possible role of ABA in the central nervous system.

Materials and Methods

Materials. See *SI Materials and Methods*.

Isolation of Human Granulocytes. Buffy coats, prepared from freshly drawn blood of healthy human volunteers, were provided by Galliera Hospital (Genoa, Italy). Granulocytes were isolated as described in ref. 9.

Fluorimetric Measurements of $[Ca^{2+}]_i$. $[Ca^{2+}]_i$ measurements were performed on freshly isolated, FURA-2-loaded granulocytes seeded on 20-mm glass coverslips, as described in ref. 9.

Determination of Intracellular cADPR Levels. Granulocytes (4×10^7/ml) were incubated for 0, 2.5, 5, 15, and 60 min at 25°C without (control) or with 20 μM ABA. At each time point, a 500-μl aliquot of the cell suspension was withdrawn and centrifuged at $5,000 \times g$ for 15 s; cell pellets were lysed in 500 μl of 0.6 M perchloric acid at 4°C. The cADPR content was measured on the neutralized cell extracts by a sensitive enzymatic cycling assay (31).

Determination of Intracellular IP$_3$ Levels. Granulocytes were resuspended in HBSS (4×10^7/ml) and exposed to 20 μM ABA with or without PTX. Aliquots (500-μl) of the suspensions were withdrawn at different times, and the reaction was stopped by adding 30 μl of 9 M perchloric acid at 4°C (31). The intracellular IP$_3$ concentration was determined by RIA (Biotrak Assay System; Amersham Bioscience AB, Milan, Italy).

Assays of ADPRC, GDP-Ribosyl Cyclase, NAD$^+$-ase and cADPR-Hydrolase Activities and Immunopurification of CD38 and Western Blot Analysis. See *SI Materials and Methods*.

Determination of Intracellular cAMP Levels. Granulocytes were resuspended in HBSS or Ca^{2+}-free HBSS (3×10^7/ml) and preincubated for 5 min at 25°C with 10 μM cAMP phosphodiesterase inhibitor 4-(3-Butoxy-4-methoxy-benzyl)imidazolidin-2-one (Ro 20-1724; Sigma, St. Louis, MO; catalog no. B8279). After incubation with or without 20 μM ABA, a 300-μl aliquot of the suspension was withdrawn at different times, and the reaction was stopped by adding 20 μl of 9 M perchloric acid at 4°C (31). The intracellular cAMP concentration was determined by RIA (Amersham Bioscience AB).

Staining of Human Granulocytes with Biotinylated ABA and Scatchard Plot Analysis of ABA-Binding Sites on Human Granulocytes. See *SI Materials and Methods*.

Phagocytosis, Determination of ROS and NO Production, Chemotaxis, and Chemokinesis. See *SI Materials and Methods*.

Detection of ABA by ELISA and by HPLC-MS. See *SI Materials and Methods*.

1. Nambara E, Marion-Poll A (2005) *Annu Rev Plant Biol* 56:165–185.
2. Lee HC, Walseth TF, Bratt GT, Hayes RN, Clapper DL (1989) *J Biol Chem* 264:1608–1615.
3. Wu Y, Kuzma J, Marechal E, Graeff R, Lee HC, Foster R, Chua NH (1997) *Science* 278:2126–2130.
4. Zocchi E, Carpaneto A, Cerrano C, Bruzzone S, Guida L, Franco L, Usai C (2001) *Proc Natl Acad Sci USA* 98:14859–14864.
5. Puce S, Basile G, Bavestrello G, Bruzzone S, Cerrano C, Giovine M, Arillo A, Zocchi E (2004) *J Biol Chem* 279:39783–39788.
6. Zocchi E, Basile G, Cerrano C, Bavestrello G, Giovine M, Bruzzone S, Guida L, Carpaneto A, Magrassi R, Usai C (2003) *J Cell Sci* 116:629–636.
7. Partida-Sánchez S, Cockayne DA, Monard S, Jacobson EL, Oppenheimer N, Garvy B, Kusser K, Goodrich S, Howard M, Harmsen A, *et al.* (2001) *Nat Med* 7:1209–1216.
8. Partida-Sánchez S, Iribarren P, Moreno-Garcia ME, Gao JL, Murphy PM, Oppenheimer N, Wang JM, Lund FE (2004) *J Immunol* 172:1896–1906.
9. Bruzzone S, Moreschi I, Guida L, Usai C, Zocchi E, De Flora A (2006) *Biochem J* 393:697–704.
10. Walseth TF, Lee HC (1993) *Biochim Biophys Acta* 1178:235–242.
11. Lee HC (2002) *Cyclic ADP-Ribose and NAADP: Structures, Metabolism and Functions* (Kluwer, Norwell, MS).
12. Gafni J, Munsch GA, Lam TH, Catlin MC, Costa LG, Molinski TF, Pessah IN (1997) *Neuron* 19:723–733.
13. Zocchi E, Franco L, Guida L, Benatti U, Bargellesi A, Malavasi F, Lee HC, De Flora A (1993) *Biochim Biophys Res Commun* 196:1459–1465.
14. Chang LC, Wang CJ, Lin YL, Wang JP (2003) *Biochim Biophys Acta* 1640:53–60.
15. Iannone MA, Wolberg G, Zimmerman TP (1991) *Biochem Pharmacol* 42:S105–S111.
16. Yamazaki D, Yoshida S, Asami T, Kuchitsu K (2003) *Plant J* 35:129–139.
17. Razem FA, Luo M, Liu J-H, Abrams SR, Hill RD (2004) *J Biol Chem* 279:9922–9929.
18. Zhang DP, Chen SW, Peng YB, Shen YY (2001) *J Exp Bot* 52:2097–2103.
19. Zhang DP, Wu ZY, Li XY, Zhao ZX (2002) *Plant Physiol* 128:714–725.
20. Vita N, Lefort S, Brouillaud MJ, Magazin M, Guillemot JC, Ferrara P (1993) *Eur Cytokine Netw* 4:197–204.
21. Razem FA, El-Kereamy A, Abrams SR, Hill RD (2006) *Nature* 439:290–294.
22. Boyer GL, Zeevaart JAD (1982) *Plant Physiol* 70:227–231.
23. Guse AH (2005) *FEBS J* 272:4590–4597.
24. Heiner I, Eisfeld J, Halaszovich CR, Wehage E, Jungling E, Zitt C, Luckhoff A (2003) *Biochem J* 371:1045–1053.
25. Kolisek M, Beck A, Fleig A, Penner R (2005) *Mol Cell* 18:61–69.
26. Di Virgilio F, Vicentini LM, Treves S, Riz G, Pozzan T (1985) *Biochem J* 229:361–367.
27. Le Page-Degivry MT, Bidard JN, Rouvier E, Bulard C, Lazdunski M (1986) *Proc Natl Acad Sci USA* 83:1155–1158.
28. Ritchie S, Gilroy S (2000) *Plant Physiol* 124:693–702.
29. Adler MW, Rogers TJ (2005) *J Leukoc Biol* 78:1204–1209.
30. Vitkovic L, Bockaert J, Jacque C (2000) *J Neurochem* 74:457–471.
31. Graeff RM, Lee HC (2002) *Biochem J* 361:379–384.